

Phase Separation from $L2_1$ to $(B2+L2_1)$ in Fe-24.6Al-7.5Ti Alloy

GowDong Tsay*¹, ChunWei Su*¹, YiHsuan Tuan*¹, ChuenGuang Chao and TzengFeng Liu*²

Department of Materials Science and Engineering, National Chiao Tung University,
1001 Ta Hsueh Road, Hsinchu 30049, Taiwan, R. O. China

As-quenched microstructure of the Fe-24.6 at% Al-7.5 at% Ti alloy was a mixture of $(A2+L2_1)$ phases. When the as-quenched alloy was aged at 1173 K for moderate times, the $L2_1$ domains grew considerably and B2 phase was formed at $a/2\langle 100 \rangle$ anti-phase boundaries (APBs) as well as phase separation from well-grown $L2_1$ to $(B2+L2_1^*)$ occurred basically contiguous to the APBs, where $L2_1^*$ is also a $L2_1$ -type phase. With continued aging at 1173 K, the phase separation would proceed toward the whole well-grown $L2_1$ domains. This microstructural evolution has not been reported in the Fe-Al-Ti alloy systems before. [doi:10.2320/matertrans.M2010167]

(Received May 12, 2010; Accepted July 16, 2010; Published September 1, 2010)

Keywords: iron aluminum titanium alloys, phase transformations, transmission electron microscopy, phase separation

1. Introduction

In previous studies,¹⁻¹¹⁾ it is seen that the Ti addition in the Fe-Al binary alloys would (1) strongly increase the $D0_3 \rightarrow B2$ and $B2 \rightarrow A2$ transition temperatures,¹⁻¹⁰⁾ (2) significantly expand the $(A2+D0_3)$ phase field,⁵⁻⁷⁾ and (3) cause the $D0_3$ APBs to exhibit a tendency toward anisotropy.⁶⁾ In addition, a $(B2+L2_1)$ ($L2_1$ is the ternary equivalent of the binary $D0_3$ structure.³⁾) two-phase field was reported to be existent at temperatures ranging from 1073 to 1273 K in the Fe-Al-Ti ternary alloys.⁷⁻¹¹⁾ It is noted that the $(B2+D0_3)$ two-phase field has not been found by previous workers in the Fe-Al binary alloys before.^{12,13)} However, the existence of the $(B2+L2_1)$ two-phase field in the Fe-Al-Ti ternary alloys was determined principally by using X-ray diffraction, differential scanning calorimetry, differential thermal analysis and electron-probe microanalysis.⁷⁻¹¹⁾ Recently, we have performed transmission electron microscopy (TEM) investigations on the phase transformations of a Fe-23 at% Al-8.5 at% Ti alloy aged at 1173 K.¹⁴⁾ Consequently, it was found that when the alloy was aged at 1173 K for longer times, the $L2_1$ domains grew considerably and an $A2 \rightarrow (A2+L2_1) \rightarrow (B2+L2_1)$ transition occurred at $a/2\langle 100 \rangle$ APBs. This feature has never been reported by other workers in the Fe-Al-Ti alloy systems before. Extending the previous work, the purpose of this study is an attempt to examine the microstructural developments of the Fe-24.6 at% Al-7.5 at% Ti alloy aged at 1173 K. It is noted that according to the previously established isothermal sections of Fe-Al-Ti ternary alloys at 1173 K,⁶⁻¹¹⁾ the chemical compositions of both the previous alloy and the present alloy are just located in the $(B2+L2_1)$ region. However, the chemical composition of the present alloy is much closer to the $A2/B2/L2_1$ apex than that of the previous alloy.

2. Experimental Procedure

The Fe-24.6 at% Al-7.5 at% Ti alloy was prepared in a vacuum induction furnace by using Fe(99.9%), Al(99.9%)

and Ti(99.9%). After being homogenized at 1523 K for 48 h, the ingot was sectioned into 2-mm-thick slices. These slices were subsequently solution heat-treated at 1373 K for 1 h and then quenched into room-temperature water rapidly. The aging processes were performed at 1173 K for various times in a vacuum heat-treated furnace and then quenched rapidly. TEM specimens were prepared by means of double-jet electropolisher with an electrolyte of 67% methanol and 33% nitric acid. Electron microscopy was performed on a JEOL JEM-2000FX scanning transmission electron microscope (STEM) operating at 200 kV. This microscope was equipped with a Link ISIS 300 energy-dispersive X-ray spectrometer (EDS) for chemical analysis. Quantitative analyses of elemental concentrations for Fe, Al and Ti were made with the aid of a Cliff-Lorimer ratio thin section method.

3. Results and Discussion

Figure 1(a) is a selected-area diffraction pattern of the as-quenched alloy, exhibiting the superlattice reflection spots of the ordered $L2_1$ phase.¹⁴⁻¹⁶⁾ Figures 1(b) and (c) are (200) $L2_1$ (or, equivalently, (100) B2) and (111) $L2_1$ dark-field (DF) electron micrographs of the as-quenched alloy, showing the presence of the small B2 domains and fine $D0_3$ domains, respectively.^{12,13)} In Figs. 1(b) and (c), it is seen that the sizes of both B2 and $L2_1$ domains are very small, indicating that these domains were formed during quenching.^{12,13)} In Fig. 1(b), it is also seen that a high density of extremely fine disordered A2 phase (dark contrast) could be observed within the B2 domains; otherwise, there would be no contrast within these domains by using a (200) superlattice reflection.⁶⁾ Accordingly, the as-quenched microstructure of the alloy was a mixture of $(A2+L2_1)$ phases. This is similar to that observed by the present workers in the Fe-23 at% Al-8.5 at% Ti alloy quenched from 1373 K.¹⁴⁾

Figure 2 is a (111) $L2_1$ DF electron micrograph of the alloy aged at 1173 K for 3 h, clearly revealing that the $L2_1$ domains grew significantly and $a/2\langle 100 \rangle$ APBs were coated with the disordered A2 phase. However, after prolonged aging at 1173 K, some tiny particles started to form within the A2 phase. A typical example is shown in Fig. 3. Figures 3(a) and (b) are (111) and (200) $L2_1$ DF electron micrographs of

*1Graduate Student, National Chiao Tung University

*2Corresponding author, E-mail: tfliu@cc.nctu.edu.tw

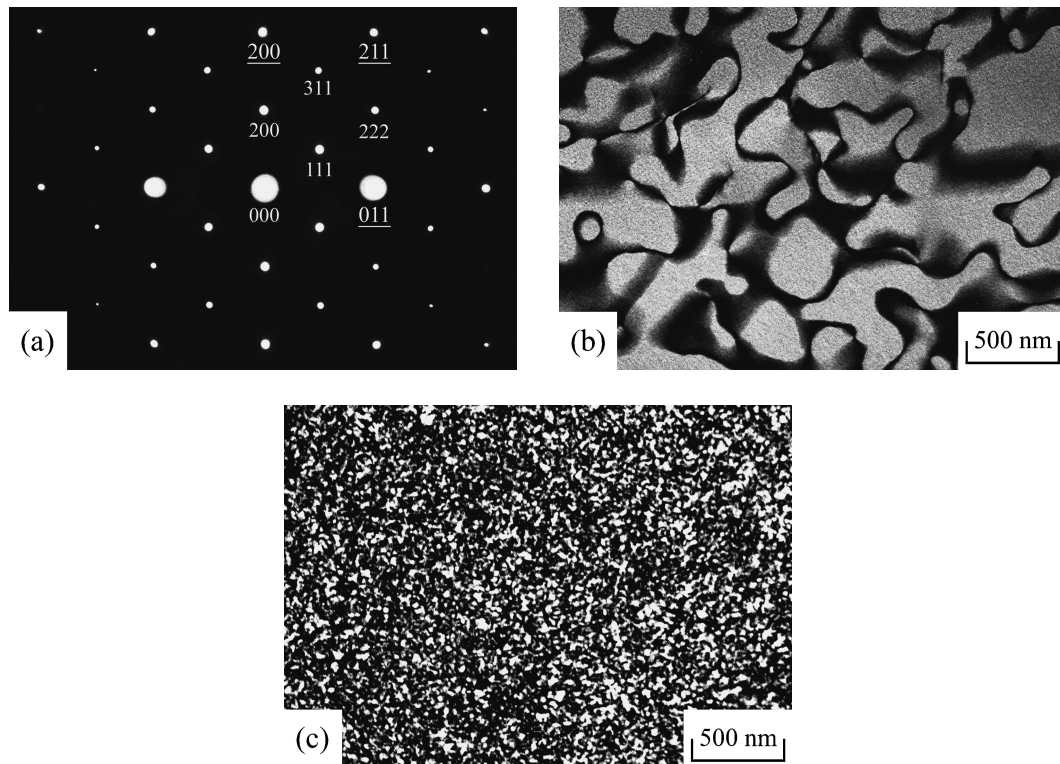


Fig. 1 Electron micrographs of the as-quenched alloy: (a) a selected-area diffraction pattern. The foil normal is $[01\bar{1}]$. (hkl : disordered A2, hkl : L_{21} phase); (b) and (c) (200) and (111) L_{21} DF, respectively.

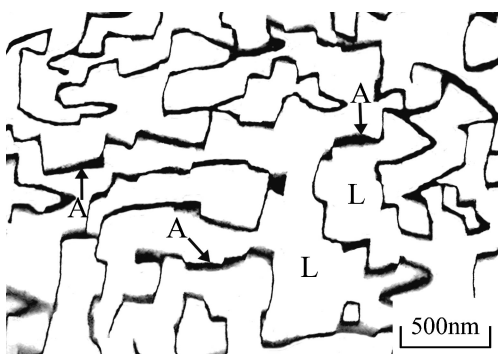


Fig. 2 (111) L_{21} DF electron micrograph of the alloy aged at 1173 K for 3 h.

the alloy aged at 1173 K for 6 h, showing that the (111) DF image and the (200) DF image are morphologically identical. Therefore, it is likely to conclude that the microstructure of the alloy aged at 1173 K for 6 h was also L_{21} phase and the $a/2\langle 100 \rangle$ APBs were coated with the disordered A2 phase. However, the (111) L_{21} DF electron micrograph of the same area as Fig. 3(a) with a higher magnification revealed that the $a/2\langle 100 \rangle$ APBs were fully dark in contrast, as shown in Fig. 3(c); whereas the (200) L_{21} DF electron micrograph showed that some tiny particles (indicated with arrows) could be observed at the $a/2\langle 100 \rangle$ APBs, as illustrated in Fig. 3(d). Therefore, it is reasonable to deduce that the tiny bright particles present in Fig. 3(d) should be of B2 phase, since the (111) reflection spot comes from the L_{21} phase only; while the (200) reflection spot can come from both the L_{21} and B2 phases.^{12,13} With continued aging at 1173 K, the L_{21} domains continued to grow and a phase separation started to

occur basically contiguous to $a/2\langle 100 \rangle$ APBs of the L_{21} domains. An example is shown in Fig. 4. Figure 4(a) is a (111) L_{21} DF electron micrograph of the alloy aged at 1173 K for 12 h, showing that the $a/2\langle 100 \rangle$ APBs broadened and well-grown L_{21} domains decomposed into fine L_{21} domains (designated as L_{21}^* phase to be distinguished from the original L_{21} phase) separated by dark layers. Figure 4(b) is a (200) L_{21} DF electron micrograph taken from the same area as Fig. 4(a), clearly revealing that in addition to the presence of a few A2 particles, the whole region is bright in contrast. This indicates that the broadened dark lines on $a/2\langle 100 \rangle$ APBs and dark layers around the periphery of the L_{21}^* domains should be of the B2 phase. It is apparent that the B2 phase was formed at $a/2\langle 100 \rangle$ APBs and phase separation from L_{21} to $(B_2+L_{21}^*)$ occurred basically contiguous to the $a/2\langle 100 \rangle$ APBs. Figure 5(a) is a (111) L_{21} DF electron micrograph of the alloy aged at 1173 K for 24 h, indicating that with increasing aging time, the phase separation would proceed toward the inside of the L_{21} domains. Figure 5(b), (200) L_{21} DF electron micrograph taken from the same area as Fig. 5(a), clearly reveals that only one $a/2\langle 100 \rangle$ APB and one A2 particle (indicated with arrows in Figs. 5(a) and (b)) could be observed. Figures 6(a) and (b) are (111) and (200) L_{21} DF electron micrographs of the alloy aged at 1173 K for 36 h, revealing that besides a little A2 phase, the well-grown L_{21} domains decomposed into the $(B_2+L_{21}^*)$ phases completely.

Based on the above observations, some important experimental results are discussed below. When the present alloy was aged at 1173 K for moderate times, the B2 phase was formed at $a/2\langle 100 \rangle$ APBs and phase separation from well-grown L_{21} to $(B_2+L_{21}^*)$ occurred basically contiguous to

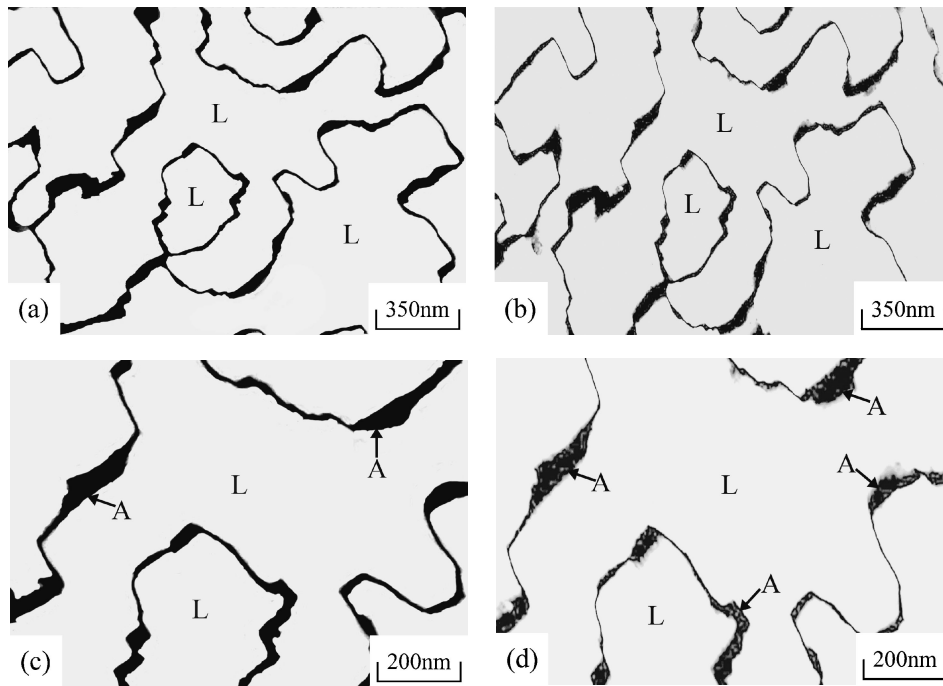


Fig. 3 Electron micrographs of the alloy aged at 1173 K for 6 h. (a) and (b) (111) and (200) L_{21} DF, respectively. (c) and (d) (111) and (200) L_{21} DF with a higher magnification of (a) and (b), respectively.

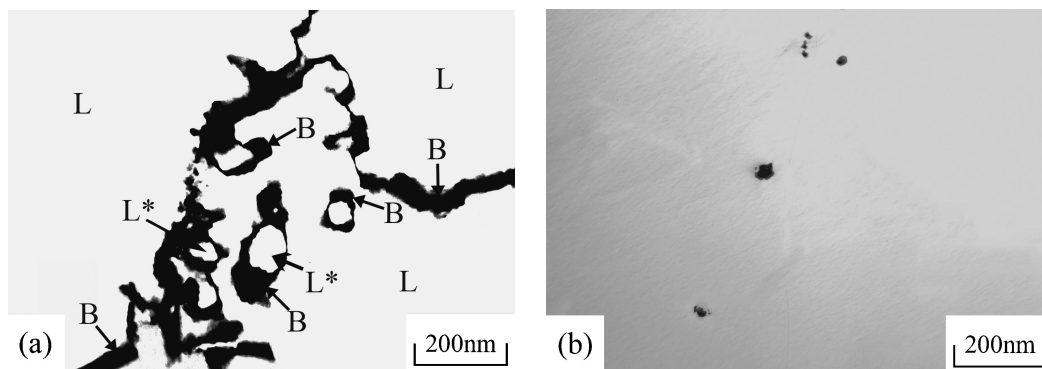


Fig. 4 Electron micrographs of the alloy aged at 1173 K for 12 h. (a) and (b) (111) and (200) L_{21} DF, respectively.

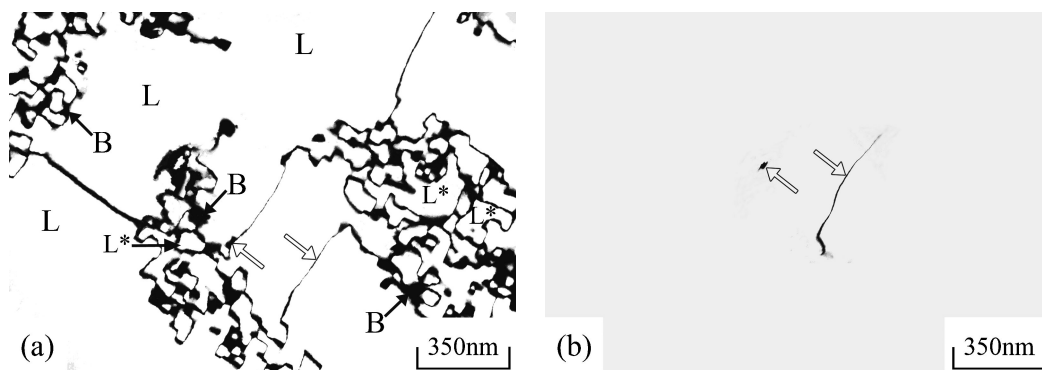


Fig. 5 Electron micrographs of the alloy aged at 1173 K for 24 h. (a) and (b) (111) and (200) L_{21} DF, respectively.

the APBs. With increased aging time at 1173 K, the phase separation would proceed toward the inside of the whole well-grown L_{21} domains. This finding is different from that observed by the present workers in the Fe-23 at% Al-8.5 at% Ti alloy,¹⁴ in which we have demonstrated that when the

Fe-23 at% Al-8.5 at% Ti alloy was aged at 1173 K, the mixture of the (B_2+L_{21}) phases occurred at $a/2\langle 100 \rangle$ APBs and no evidence of the phase separation could be observed. In order to clarify the apparent difference, an STEM-EDS study was undertaken. The EDS analyses were taken from the

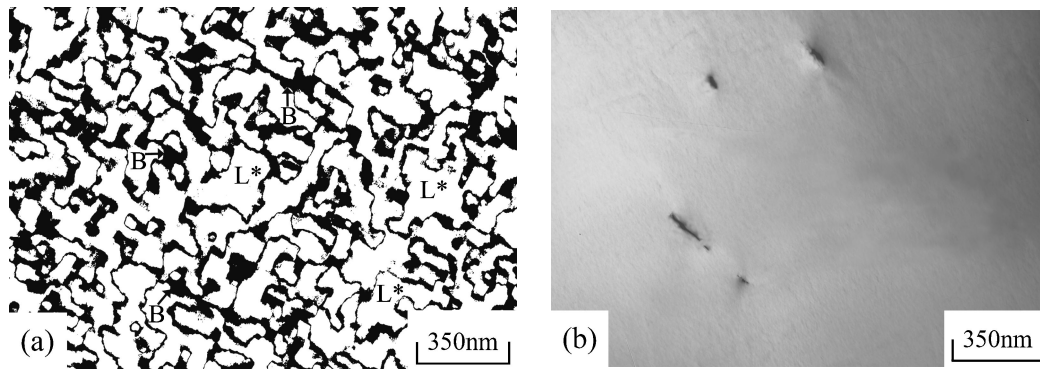


Fig. 6 Electron micrographs of the alloy aged at 1173 K for 36 h. (a) and (b) (111) and (200) L₂₁ DF, respectively.

Table 1 Chemical compositions of the phases revealed by EDS.

Heat treatment	Phase	Chemical composition (at%)		
		Fe	Al	Ti
As-quenched	A2+L ₂₁	67.9	24.6	7.5
1173 K, 3 h	L ₂₁	65.9	26.2	7.9
	APB(A2)	76.4	19.8	3.8
1173 K, 6 h	L ₂₁	66.5	25.7	7.8
	APB(A2+B2)	74.0	22.1	3.9
1173 K, 12 h	L ₂₁	67.0	25.2	7.8
	L ₂₁ *	66.2	25.1	8.7
	B2	69.6	24.1	6.3
1173 K, 24 h	L ₂₁	67.2	25.1	7.7
	L ₂₁ *	66.2	25.0	8.8
	B2	69.6	24.2	6.2
1173 K, 36 h	L ₂₁ *	66.1	25.1	8.8
	B2	69.5	24.2	6.3

areas of the L₂₁ domains, APBs, B2 phase and L₂₁* domains marked as “L”, “A”, “B” and “L*” in Figs. 2 through 6, respectively. The average concentrations of the alloying elements obtained by analyzing at least ten different EDS spectra of each phase are listed in Table 1. For comparison, the chemical composition of the as-quenched alloy is also listed in Table 1. It is clearly seen in Table 1 that when the alloy was aged at 1173 K for 3 h, the Al and Ti concentrations in the L₂₁ domains were distinctly higher than those in the as-quenched alloy. This means that along with the growth of the L₂₁ domains, the concentrations of both Al and Ti at a/2⟨100⟩ APBs would be lacking. The insufficient concentrations of both Al (19.8 at%) and Ti (3.8 at%) would cause the disordered A2 phase to form at a/2⟨100⟩ APBs, which is consistent with the previously established Fe-Al-Ti phase diagram as shown in Fig. 7.¹⁰ According to the phase diagram, the chemical composition of Fe-19.8 at% Al-3.8 at% Ti is just located in the A2 phase region. EDS analyses indicated that when the alloy was aged at 1173 K for 3–12 h, the Ti concentration in the L₂₁ domains maintained to be about 7.8 at% and the Al concentration gradually decreased with increasing the aging time. It is thus expected that the Al atom would proceed to diffuse toward the a/2⟨100⟩ APBs during aging. In Table 1, it is seen that when

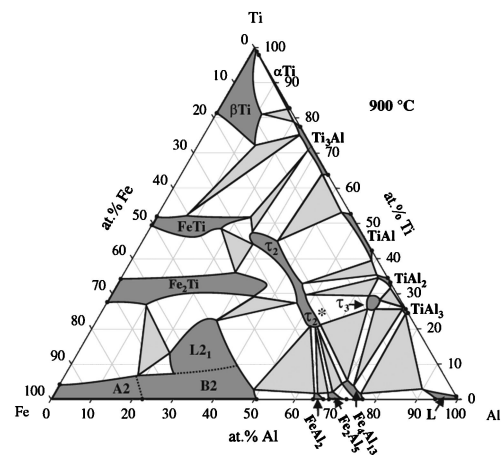


Fig. 7 Isothermal section of the Fe-Al-Ti system at 1173 K.¹⁰

the alloy was aged at 1173 K for 6 h, the Al concentration at a/2⟨100⟩ APBs increased to 22.1 at%. The significant increase of the Al concentration would lead the tiny B2 particles to form at a/2⟨100⟩ APBs, which is also consistent with the Fe-Al-Ti phase diagram in Fig. 7.¹⁰ In the phase diagram, it is clearly seen that the chemical composition of Fe-22.1 at% Al-3.9 at% Ti is close to the A2/B2 transition boundary. With increasing the aging time, the L₂₁ domains continued to grow. The quantitative analyses revealed that the Al concentration of the L₂₁ domains in the alloy aged for 6 h was 25.7 at% while that for 12 h was 25.2 at%, which gave a decrease of only 0.5 at%. However, along with the enlargement of the L₂₁ domain size, the volume fraction of the a/2⟨100⟩ APBs would be lessened considerably. This means that the slight decrease of the Al concentration in the L₂₁ domains would cause the Al concentration at a/2⟨100⟩ APBs to increase appreciably. Therefore, it is reasonable to believe that due to the appreciable increase of the Al concentration, the A2 phase existing at a/2⟨100⟩ APBs would be transformed to B2 phase,¹⁰ as observed in Fig. 4(a). TEM observations indicated that along with the formation of the B2 phase, the phase separation from well-grown L₂₁ to (B2+L₂₁*) occurred basically contiguous to a/2⟨100⟩ APBs. In the following description, we will attempt to discuss why the well-grown L₂₁ domains underwent the phase separation. In the previous studies, it is well-known that the DO₃ phase could be found to exist in the Fe-Al binary

alloys only at temperatures below 823 K,^{12,13)} and the Ti addition in the Fe-Al binary alloys would result in a particularly large increase of the $D0_3(L2_1) \rightarrow B2$ transition temperature about 60 K/at%.⁶⁻¹¹⁾ Obviously, the Ti concentration would be the predominant factor for the stabilization of the $L2_1$ phase at high temperature. In our previous study of the Fe-23 at% Al-8.5 at% Ti alloy aged at 1173 K for 6–24 h,¹⁴⁾ it was found that the Ti concentration in the well-grown $L2_1$ domains was up to about 11.1 at%, therefore, the $L2_1$ phase exhibited more stable and no evidence of the phase separation could be detected. However, when the present alloy was aged at 1173 K for 6–24 h, the Ti concentration in the well-grown $L2_1$ domains was found to be only about 7.8 at%, which is noticeably lower than that detected in the previous alloy. Therefore, it is plausible to suggest that owing to the lower Ti concentration, the well-grown $L2_1$ domains seemed not very stable at 1173 K. Consequently, the well-grown $L2_1$ domains would separate to the mixture of the Ti-riched $L2_1^*$ and Ti-lacked B2 phase, as observed in Figs. 4 through 6.

Finally, three more features are worthwhile to note as follows: (1) In the previous study,¹⁴⁾ it is clearly seen that the $a/2\langle 100 \rangle$ APBs of the well-grown $L2_1$ domains exhibited more pronounced anisotropy than those observed in the present alloy. The reason is possibly that the well-grown $L2_1$ domains in the previous alloy had significantly higher Ti concentration. (2) The chemical composition of the previous alloy had higher Ti and lower Al contents.¹⁴⁾ When the previous alloy was aged at 1173 K, the $L2_1$ domains grew rapidly and the Ti atom was the major element for diffusing into the $a/2\langle 100 \rangle$ APBs. This effect caused the tiny $L2_1$ particles to precipitate preferentially at $a/2\langle 100 \rangle$ APBs.¹⁴⁾ However, when the present alloy was aged at 1173 K, the Ti concentration in the well-grown $L2_1$ domains maintained to be about 7.8 at% and the Al atom played the dominant role to diffuse into the $a/2\langle 100 \rangle$ APBs. Therefore, the tiny B2 particles were found to form at the $a/2\langle 100 \rangle$ APBs, rather than $L2_1$ particles. (3) According to the Fe-Al-Ti phase diagrams,⁶⁻¹¹⁾ the A2 phase can not appear for the Fe-24.6 at% Al-7.5 at% Ti alloy. However, a little A2 phase was always observed in the present alloy aged at 1173 K for 12–36 h. The reason for the difference is plausibly that the phase diagrams were determined by the Fe-Al-Ti alloys heat-treated at 1173 K for a time period longer than 336 h, whereas the present alloy was aged for 36 h only. Actually, in the

present study, it was found that when the as-quenched alloy was aged at 1173 K for 3–36 h, the amount of the A2 phase was indeed decreased with increasing the aging time.

4. Conclusions

In the as-quenched condition, the microstructure of the Fe-24.6 at% Al-7.5 at% Ti alloy was the mixture of ($A2+L2_1$) phases. When the as-quenched alloy was aged at 1173 K for 6 h, the $L2_1$ domains grew considerably and the B2 phase was formed at $a/2\langle 100 \rangle$ APBs as well as the phase separation from well-grown $L2_1$ to ($B2+L2_1^*$) occurred basically contiguous to the $a/2\langle 100 \rangle$ APBs. After prolonged aging at 1173 K, the phase separation would proceed toward the inside of the whole well-grown $L2_1$ domains. Consequently, the microstructure of the alloy aged at 1173 K for 36 h was essentially the mixture of ($B2+L2_1^*$) phases.

Acknowledgment

This work was supported by the National Science Council, Taiwan (NSC-97-2221-E-009-027-MY3).

REFERENCES

- 1) Y. Nishino, S. Asano and T. Ogawa: *Mater. Sci. Eng. A* **234–236** (1997) 271–274.
- 2) F. Stein, A. Schneider and G. Frommeyer: *Intermetallics* **11** (2003) 71–82.
- 3) M. Palm: *Intermetallics* **13** (2005) 1286–1295.
- 4) L. Anthony and B. Fultz: *Acta Metall. Mater.* **43** (1995) 3885–3891.
- 5) O. Ikeda, I. Ohnuma, R. Kainuma and K. Ishida: *Intermetallics* **9** (2001) 755–761.
- 6) M. G. Mendiratta, S. K. Ehlers and H. A. Lipsitt: *Metall. Trans. A* **18** (1987) 509–518.
- 7) I. Ohnuma, C. G. Schon, R. Kainuma, G. Inden and K. Ishida: *Acta Mater.* **46** (1998) 2083–2094.
- 8) S. M. Zhu, K. Sakamoto, M. Tamura and K. Iwasaki: *Mater. Trans.* **42** (2001) 484–490.
- 9) M. Palm and G. Sauthoff: *Intermetallics* **12** (2004) 1345–1359.
- 10) M. Palm and J. Lacaze: *Intermetallics* **14** (2006) 1291–1303.
- 11) G. Ghosh: G. Effenberg (Ed.), *Ternary Alloy Systems*, (Springer, Berlin, 2005) pp. 426–452.
- 12) P. R. Swann, W. R. Duff and R. M. Fisher: *Metall. Trans.* **3** (1972) 409–419.
- 13) S. M. Allen and J. W. Cahn: *Acta Metall.* **24** (1976) 425–436.
- 14) C. W. Su, C. G. Chao and T. F. Liu: *Scr. Mater.* **57** (2007) 917–920.
- 15) S. Y. Yang and T. F. Liu: *Scr. Mater.* **54** (2006) 931–935.
- 16) C. H. Chen and T. F. Liu: *Metall. Trans. A* **34** (2003) 503–509.